Carbohydrate Polymers 79 (2010) 373–379

Contents lists available at ScienceDirect

Carbohydrate Polymers

journal homepage: www.elsevier.com/locate/carbpol

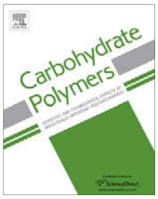

# Synthesis and properties of silicone/montmorillonite nanocomposites by in-situ intercalative polymerization

Xinhua Yuan *, Xiaohui Li, Enbo Zhu, Jie Hu, Shunsheng Cao, Weichen Sheng

*School of Material Science and Engineering, Jiangsu University, Zhenjiang, Jiangsu, 212013, People's Republic of China*

ARTICLE INFO

*Article history:*
Received 16 July 2009
Received in revised form 6 August 2009
Accepted 13 August 2009
Available online 18 August 2009

*Keywords:*
Montmorillonite
Silicone
In-situ intercalative polymerization
Nanocomposites
Preparation

ABSTRACT

Using cetyltrimethylammonium bromide (CTAB) as organic treatment agent, phenylmethylsilicone/organic montmorillonite (OMMT) nanocomposites were prepared by in-situ intercalative polymerization. The internal structure and morphology of the nanocomposites were characterized by X-ray diffraction (XRD), scanning electron microscope (SEM) and transmission electron microscope (TEM). Mechanical properties, high temperature resistance and barrier performance for gas and water were also studied. The results show that molecules of silicone chains insert into the layer of montmorillonite (MMT), and the interlayer distance of MMT is expanded effectively after polymerization of phenylmethylsilicone prepolymer and methyl methacrylate, even forming exfoliated nanocomposites. The silicone/OMMT nanocomposite containing 8 wt% OMMT has better high temperature resistance and barrier properties with low thermal weight loss of 25% at 750 °C. The nanocomposite, containing 6 wt% OMMT, has better mechanical performance with tension strength of 6.264 MPa, which is five times more than that of pure silicone. When the nanocomposite contains 4 wt% OMMT, the compression strength is 11.503 MPa, which is four times bigger than that of pure silicone.

## 1. Introduction

During the last 10 years, preparation and characterization of organic–inorganic nanocomposites have attracted a great deal of attention in material science (Akat, Tasdelen, Prez, & Yagci, 2008; Chiu, Lai, Chen, & Lee, 2005; Dasari, Yu, & Mai, 2005; Deshmane, Yuan, & Misra, 2007; Fornnes & Paul, 2003; Huang, Yu, & Ma, 2006; Huskic & Zigon, 2007; Incarnato, Scarfato, Scatteia, & Acierno, 2004; Luo & Daniel, 2003; Wagener & Reisinger, 2003; Yang & Hu, 2006; Yuan & Misra, 2006). They are of interest both from fundamental academic research aspect and industrial applications, due to their potentials to advanced properties at very low filler concentrations only a fraction of that typically required by conventional fillers (Chiu et al., 2005; Fornnes & Paul, 2003). Among the different nanoparticles used in polymer nanocomposites, clay or MMT has been extensively used, because of low cost and good mechanical properties (Deshmane et al., 2007; Yang & Hu, 2006; Yuan & Misra, 2006). In addition, the ability of the silicate particles to disperse into individual layers in polymeric matrix and ability to fine tune their surface reactions, resulting in excellent mechanical and physical property enhancements of polymer/MMT nanocomposites (Akat et al., 2008; Dasari et al., 2005; Deshmane et al., 2007; Huskic & Zigon, 2007). Polymer/MMT nanocomposites have been successfully prepared by intercalating polymers into MMT. According to the starting materials and process techniques, the preparation methods of polymer/MMT nanocomposites are divided into three main groups: solution intercalation of polymer or prepolymer, in-situ intercalative polymerization and melt intercalation (Morgana & Harrisb, 2004). Depending on the degree of penetration of the polymer chains into the interlayer space, intercalated and exfoliated nanocomposites are distinguished (Homminga, Goderis, Dolbnya, & Groeninckx, 2006). Nylon-6/MMT nanocomposites were firstly synthesized and commercialized by Toyota research group (Usuki et al., 1993). This nanocomposite material was prepared by in-situ polymerization method (Kojima et al., 1993; Usuki et al., 1993). The monomer was used as solvent for swelling the clay, and followed by polymerization of monomer to obtain polymer chains between the intercalated sheets (Kojima et al., 1993; Usuki et al., 1993; Zanetti, Lomakin, & Camino, 2000).

MMT was dispersed in distilled water which contained additives and acrylamide, and poly-(acrylamide)/MMT nanocomposite was prepared by UV or electron beam irradiation polymerization (Gao, Robert, Berthod, & Li, 2005). Characterization of FT-IR, XRD and NMR show that acrylamide intercalates into MMT interlayer and enlarges the layers space of MMT from 1.25 nm to 2.09 nm. By intercalating ammonium cations of polyoxyalkylene (Jeffamine) through an ion exchange process, Salahuddin (2004) prepared organoclays to synthesize epoxy-clay nanocomposites. Polyoxy-

---

* Corresponding author. Tel.: +86 511 88791409; fax: +86 511 88791947.
*E-mail address:* yuanxh1975@yahoo.com.cn (X. Yuan).

0144-8617/$ - see front matter © 2009 Elsevier Ltd. All rights reserved.
doi:10.1016/j.carbpol.2009.08.014

propylene triamine (Jeffamine T-403), primary polyethertriamine (Jeffamine T-5000) and three types of polyoxypropylene diamine (Jeffamine D-230, D-400, D-2000) with different molecular weight were used to treat Na-montmorillonite (MMT) to form organoclays. The preparation involves the ion exchange of $Na^+$ in MMT with the organic ammonium group in Jeffamine compounds. X-ray diffraction (XRD) confirms the intercalation of these organic moieties to form Jeffamine–MMT intercalates. The hardness of all nanocomposites is enhanced with the inclusion of organoclay. The toughness decreases or does not change with the inclusion of organoclay. However, the solution intercalation technology has its limitations because it may be difficult to obtain a suitable monomer to intercalate into MMT layers or a suitable solvent to dissolve polymer and disperse MMT.

Silicone has many excellent properties, such as high temperature resistance, weatherability, hydrophobic property, electrical insulation, but with poor solvent resistance and mechanical properties. Polymer/clay nanocomposites can solve these problems. Several studies have reported about silicone rubber/MMT nanocomposites (Dong et al., 2006; Kaneko & Yoshida, 2008; Kim, Kim, Shim, & Yoon, 2008). However, there are few studies about silicone/clay nanocomposite. In the present research, the solvent of toluene and methylphenyl silicone prepolymer were used to intercalate OMMT layers to prepare silicone/OMMT nanocomposites by in-situ intercalative polymerization. The preparation conditions are moderate. The thermal stability and dimensional stability of composite can be significantly improved since clay layers are dissected well in silicone. The internal structure and morphology of the nanocomposites were characterized by XRD, SEM and TEM analyses. Mechanical properties, high temperature resistance and barrier performance for water were also studied.

## 2. Experimental

### 2.1. Materials

Phenylmethylsilicone (UN6302) was purchased from Shanghai United Chemicals & New Materials Co., Ltd., (Shanghai, China). Sodium montmorillonite (Na-MMT) was provided by Zhejiang Fenghong Clay Chemicals Co., Ltd., (Zhejiang, China). Triethanolamine, methyl methacrylate (MMA), benzoperoxide (BPO), toluene were purchased from Sinopharm Chemical Reagent Co., Ltd., (Beijing, China) and were used without further purification. CTAB was obtained from Jining Chemical Institute (Jining, China).

### 2.2. Preparation of organo-MMT and silicone/OMMT nanocomposites

#### 2.2.1. Preparation of OMMT

The intercalation of CTAB into MMT was achieved by the cation exchange of Na cation with organic ammonium group in CTAB according to the following general procedure. In 400 mL distilled water, 15 g of Na-MMT was suspended and stirred for several hours at room temperature. The mixture of hydrochloric acid and CTAB ($n_{\mathrm{CTAB}}:n_{\mathrm{HCl}} = 1:1$) was slowly added with continued stirring. The mixture was then stirred for an additional 24 h at 80 °C. The precipitate was filtered, washed with distilled water for several times until no bromide ions were detected in the filtrate by testing with $AgNO_3$ (0.1 mol/L). The resultant product was dried in vacuum at 60 °C until constant weight. The final product was ground into powder in a mortar and sieved with 400-mesh sieve.

#### 2.2.2. Preparation of silicone/OMMT nanocomposites

In a two-neck (250 mL) flask equipped with a stirrer, nanocomposites were prepared by first swelling the desired concentration of dry modified MMT with toluene, phenylmethylsilicone and MMA by stirring for 0.5 h at 75 °C using water bath heating method. In order to obtain complete diffusion of phenylmethylsilicone and MMA molecules in OMMT layers, the mixture was stirred for another 0.5 h under ultrasonic condition. The reaction system was taken into water bath again and stirred for 1.5 h at 75 °C after suitable amount of BPO was added. BPO can induce MMA polymerization. After drying in a vacuum oven at 60 °C for 1.5 h, the mixture was heated to 95 °C with continuous stirring. Triethanolamine, the curing agent, was added and the reaction system was stirred for an additional 5 min. The curing mechanism was explained in Fig. 1. The mixture was poured into a home-made open rectangular mold with dimension (110) mm × (80) mm and (15) mm thickness, followed by curing process in a vacuum oven at 90 °C for 36 h. Finally, the polymer/OMMT (Polymer/layered Silicate, PLS) nanocomposites were obtained.

### 2.3. Measurements and characterizations

#### 2.3.1. Morphological analysis

Wide-angle X-ray diffraction (WXRD) measurement was carried out using D/max 2500VB3+/PC (Rigaku, Japan) equipped with a Ni-filtered monochromatic Cu-Kα radiation ($\lambda = 1.5418$ Å) at a scanning rate of 1°/min and divergence slit 1°. Measurements were made to examine the interlayer activity in the composite as prepared. The plates of silicone/OMMT nanocomposites which were produced during the molding process have smooth surface. Therefore a rectangle shaped specimen (10 mm × 5 mm × 1 mm) were cut from these plates and directly analyzed by X-ray analysis. Bragg's Law ($n\lambda = 2d\sin\theta$) was used to calculate the crystallographic spacing. A JEOL JSM-6480 (Japan) scanning electron microscope was used to observe the particle size of MMT and particle-matrix adhesion in the cured composite on the fracture surface. The specimens were coated by gold. TEM analysis was used to confirm the morphological information obtained from the XRD data on the platelet dispersion and distribution. The morphology can not be fully characterized only by XRD analysis. The absence of scattered intensity peaks in the XRD diagrams can not always surely demonstrate achievement of the disordered intercalated or the exfoliated structures. The ultra-thin TEM specimens from the powder of specimen were immersed in the alcohol and dispersed by ultrasonic. The solution was dripped on copper grids to be viewed with a JEOL JEM-2100 electron microscope at an accelerating voltage of 200 kV.

#### 2.3.2. Thermal analysis

Differential scanning calorimetric (DSC) data were taken with a Netzsch PHOENIX DSC204 instrument. About 10 mg of the sample was used to be encapsulated in aluminum pans. The measurements were conducted in the temperature range of 303–923 K. A scan speed of 10 K/min was used in the measurements. Thermogravimetric (TG) data were acquired with a Netzsch STA 409 instrument.

#### 2.3.3. Measurements of barrier properties for water

To determine barrier properties of water, rectangle shaped specimens (20 mm × 8 mm × 2 mm) of silicone /OMMT nanocomposites were made. The specimens were heated in deionized water at 80 °C for 0.5 h. Water adsorption rate ($a$) was used to denote barrier property of water and defined as follows:

$$a = \frac{m_2 - m_1}{m_1} \times 100\%$$

where, $m_1$ (g) and $m_2$ (g) represent the weight of specimen before and after boiled, respectively.

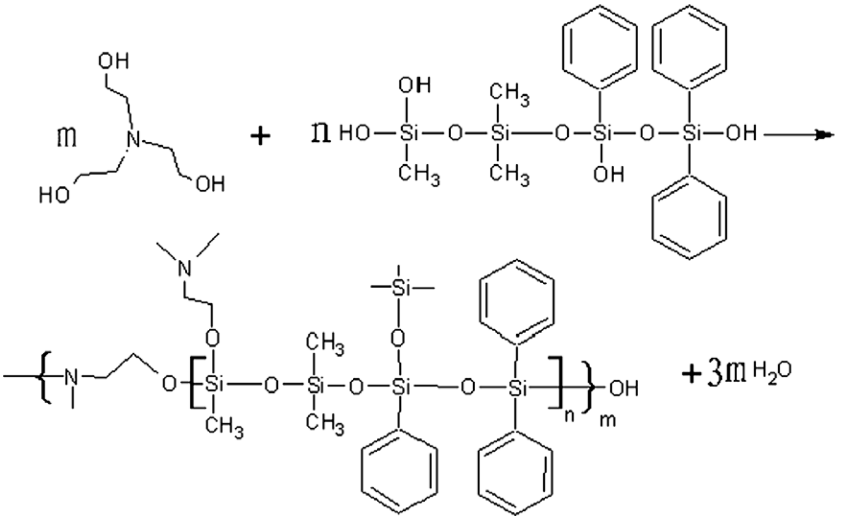

**Fig. 1.** Schematic diagram of curing reaction for phenylmethylsilicone in the layer of OMMT.

*2.3.4. Mechanical properties*

The tensile test was conducted on WDS electronic tensile testing machine (Chengde Precision Testing Machine Co., Ltd., China) at room temperature. The test specimens were cut in the shape 100 mm × 10 mm × 4 mm. Five samples were tested and the average value was taken. The tensile test speed was 5 mm/min. The compressive test was taken on WDW-11 Computer-controlled electronic universal testing machine (Jinan Shidai Shijin Instrument Co., Ltd., China), and the loading rate is 2 mm/min. All five samples were shaped for 30 mm × 10 mm × 4 mm and the compression strength was taken by average value.

## 3. Results and discussion

### 3.1. Organically modified MMT

Fig. 2(A) and (B) show the XRD spectra of the MMT and OMMT. X-ray diffraction data of the products indicate that the hydrophilic nature of Na-MMT allows the CTAB molecules to migrate between the layers. The high surface energy of the clay attracts polar species molecules so that they diffuse in between the layers during the cation exchange process. The peak in XRD patterns corresponds to the (0 0 1) reflection peak of layered silicate. In Fig. 2, the *d*-spacing of MMT calculated using Bragg's Law is about 15.61 Å on a base of $2\theta = 5.66$. For the organo-MMT, the characteristic (0 0 1) peak of the MMT shifted to a lower angle of $2\theta = 3.74$, which corresponds to *d*-spacing of 23.62 Å. It seems that, because of ion-exchanging of organic ammonium cations of CTAB with $Na^+$ cations of MMT, the parallel stacking of nanofiller is partially disrupted. The intercalation of CTAB makes the basal spacing of MMT layers become larger and changes the micro-environment of MMT layers from hydrophilic nature to hydrophobic nature, so that OMMT is suitable for the intercalation of organic molecules of prepolymer and silicone.

### 3.2. Silicone/OMMT nanocomposites morphological characterization

There is no diffraction peak at the angle region of 3–10°. To confirm this result, small-angle X-ray diffraction (SXRD, 1–10°) measurement was carried out using D/max 2500VB3+/PC (Rigaku, Japan) equipped with a Ni-filtered monochromatic Cu-Kα radiation ($\lambda = 1.5418$ Å) at a scanning rate of 1°/min for nanocomposite. The SXRD spectrum of PLS nanocomposite was given in fig. 2(C). There is no diffraction peak at low angle region of 1–10°, which means that the *d*-spacing of OMMT within the nanocomposite is at least over 80 Å. This result indicates that molecules of silicone chains have intercalated into the layers of MMT, and the interlayer distance of MMT is expanded effectively after polymerization of phenylmethylsilicone prepolymer and methyl methacrylate, even forming exfoliated nanocomposites.

MMT characterized by morphological hierarchy comprising lamellar assembly into primary particles which amass into aggregates. Since nanostructures cannot simply be deduced from change of *d*-spacing measurements that detect lamellar activity, the fracture surfaces of silicone/OMMT (6 wt%) nanocomposite were observed by SEM spectrum. Searching for mineral domains at the fracture surface of nanocomposite (Fig. 3) reveals the absence of large mineral aggregates. This suggests that the mineral domains are submicron in size. It can be concluded that OMMT and silicone are compatible very well from the SEM spectrum, which also means that each lamella of MMT has been dispersed well in polymer matrix. However, some pores with about 10 μm diameter can be seen in SEM image. These pores may be due to the solvent evaporation and will affect mechanical performance of nanocomposites.

The most powerful and direct evidence to describe whether the nanocomposite is exfoliated or intercalated is by means of TEM. TEM spectrum of a thin film of OMMT/silicone nanocomposite is shown in Fig. 4. The overall picture shows that the MMT layers are not occupying the full volume and large regions of pure silicone are visible. The molecules of silicone chains have inserted into the interlayer of MMT, forming the structure of light and dark stripes. Dark lines corresponding to several clay layers (multiplets) with an average thickness of 5 nm were observed. The distance between these multiplets is around 100 Å. The data illuminates that the absence of 0 0 1 reflection may be caused by a wider distribution of layer spacing. The layers are not entirely orderly intercalative structure in the whole region, but basically orderly and partially exfoliated morphology. Most of organo-MMT exists in nanocomposite with bending status, which illuminates that montmorillonite expresses somewhat flexible under external force and can bear some deformation.

### 3.3. Barrier property for water

Comparing to pure polymer or mechanical blending composites, PLS nanocomposites has better barrier properties for gas and

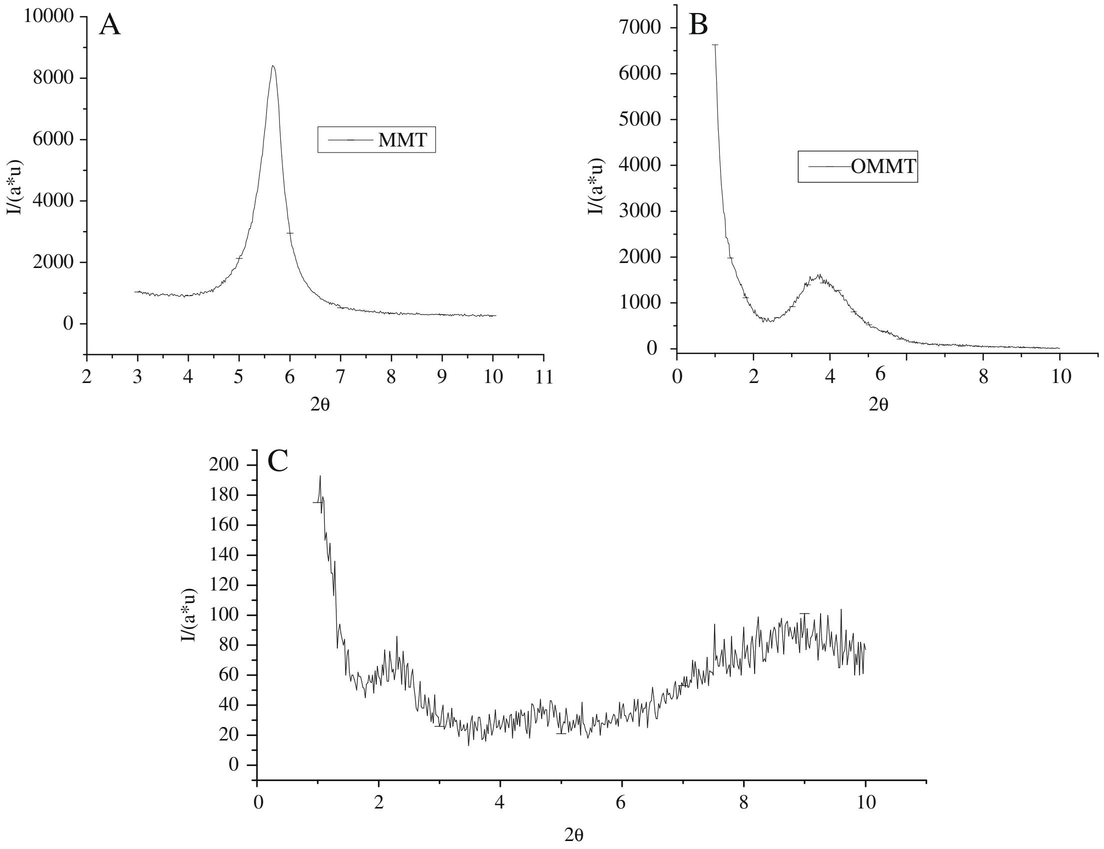

**Fig. 2.** XRD spectrum ((A) MMT; (B) OMMT; (C) SXRD spectrum of PLS nanocomposite containing 6 wt% OMMT).

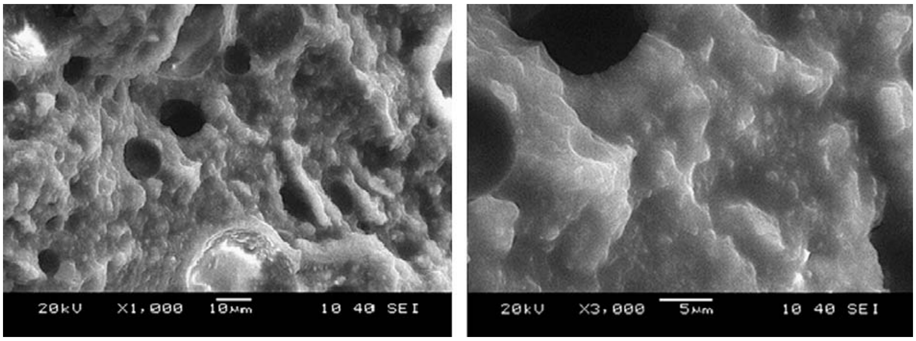

**Fig. 3.** SEM spectra of fracture surface from PLS nanocomposite containing 6 wt% OMMT.

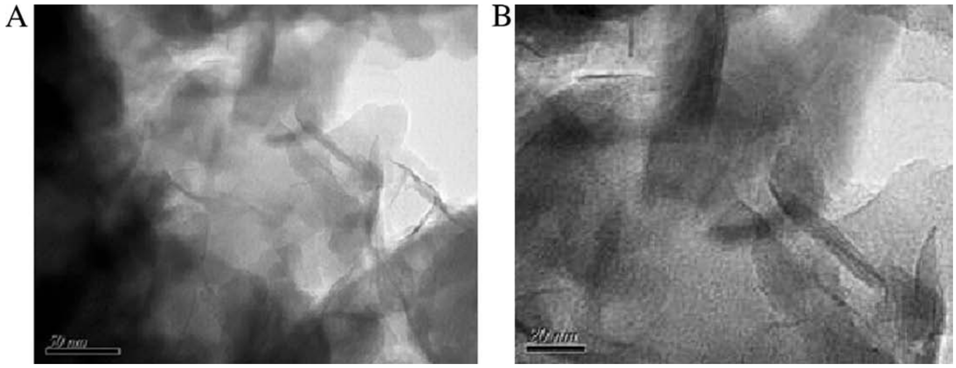

**Fig. 4.** TEM micrograph of thin sections of fully cured silicone/OMMT nanocomposite containing 6 wt% OMMT. (A) low magnification; (B) high magnification.

liquid. This may be due to the fact that the silicate layers have a large aspect ratio. When these layers of MMT well disperse in polymer matrix, the diffusion movement of gas or liquid molecules has to bypass these silicate layers. Therefore, the increase of efficient paths enhances the barrier properties for gas and liquid. The mechanism can be simply explained by Fig. 5.

In the A film, the whole material is made of polymer chain and forms a homogeneous system. The molecules of gas or liquid can pass A film from one side to another side through the free space between the polymer chains, which dotted as shown in Fig. 5A. Therefore, the barrier properties for gas and liquid of pure polymer film are usually poor. However, in the B film, because the matrix is filled with the silicate layers with a large aspect ratio and the silicate layers disperse well in polymer matrix at nano-size. The diffusion movement of gas molecules or liquid molecules has to bypass these silicate layers, twists and turns on the dotted line as shown in fig. 5B. The equivalent path will be increased markedly. If the thickness of thin film is *d*, the width and thickness of layered silicate's layer are *L* and *W*, respectively, the efficient path of $d_{\mathrm{PLS}}$ for PLS nanocomposite thin film can be calculated as follows (Qi & Shang, 2002):

$$d_{\mathrm{PLS}} = d + d\frac{L \bullet V_f}{2W} \quad (1)$$

The relationship curve of water adsorption rate and OMMT content is described in Fig. 6. The water absorption rate basically decreases with the increasing of OMMT content, which indicates that the barrier property for water of silicone/OMMT nanocomposites is increased. This conclusion is coincident with Eq. (1). The silicone/OMMT nanocomposites in the study were prepared by in-situ solution intercalative polymerization. Therefore, solvent evaporation may leave some pores in nanocomposites which were presented in SEM images of Fig. 3. These pores will obviously affect the barrier property of nanocomposites, so that the curve of the water absorption rate vs. OMMT content is not linear which should be linear according to Eq. (1). When the silicone/OMMT nanocomposite contains OMMT over 4 wt%, the barrier property for water hardly changes. This maybe due to that only intercalation or exfoliated nano-film layer can play a role to barrier property for water, and micron or submicron particles have no barrier effect on barrier property.

### 3.4. Thermal property

TGA analyses of silicone/OMMT nanocomposites with different OMMT content are shown in Fig. 7. In the initial stage of heating in the temperature range 100–360 °C, except for nanocomposite containing 8 wt% OMMT, other nanocomposites degrade slightly faster than pure silicone causing a slight weight loss. In the later stage above 360 °C, the overall thermal resistances of nanocomposites are higher than that of pure silicon. The silicone/OMMT nanocomposite containing 8 wt% OMMT has excellent temperature resistance, which can be seen from Fig. 7 that the weight losses are only 10% at 410 °C and 25% at 750 °C, respectively. However, the weight losses of other nanocomposites are all more than 20% at 410 °C. Among these composites, the thermal property of the nanocomposite containing 10 wt% OMMT is the worst, and the weight loss reaches 35% at 460 °C. When the temperature is above 460 °C, the thermal resistance becomes higher than that of pure silicone. It seems that OMMT content plays a great effect on the temperature resistance of nanocomposite. The improvement in the decomposition temperature in the new materials is attributed to the presence of a constrained region in the nanocomposite. During combustion, the flammable small molecules which come from the degradation of polymer chains are slowed down and obstructed to move to the combustion interface by the layers of layered silicate. At the same time, the layers of layered silicate can also slow down the outside oxygen to penetrate into the internal nanocomposite and the combustion at interface cannot be fully carried out. The layered silicate disperses well in polymer matrix at nano-size, which means that minimal amount can disperse through the whole silicone matrix. The silicone chains which insert into MMT are strongly restricted by the nano-space between the layers of layered silicate. If two or more molecule chains of polymer matrix pass through the nano-space, the layers of silicate will play a role of physical association for the whole PLS nanocomposite to maintain its initial shape and to enhance the thermal resistance. Therefore, the temperature resistance enhances from C to F nanocomposite with the increasing of OMMT content as shown in Fig. 7. However, when the OMMT content is over 8 wt%, the thermal

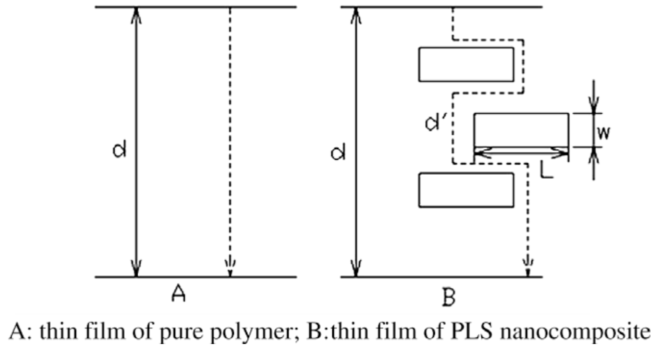

A: thin film of pure polymer; B:thin film of PLS nanocomposite

**Fig. 5.** Schematic diagram of barrier properties for gas and liquid.

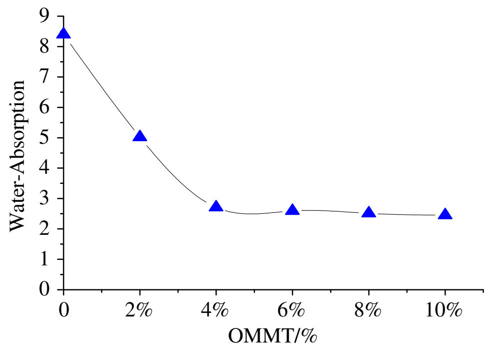

**Fig. 6.** Effect of OMMT content on the barrier properties for water.

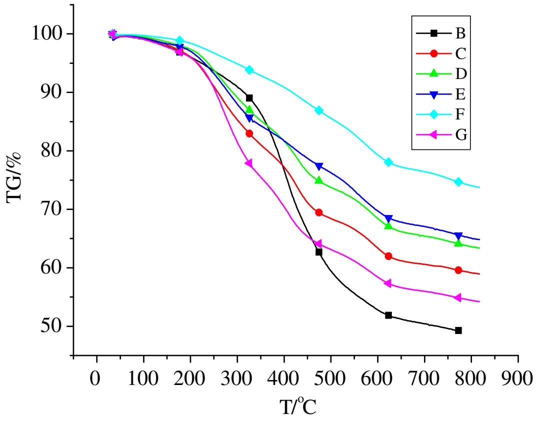

**Fig. 7.** TGA curves for silicon/OMMT nanocomposites with various modified clay content. OMMT content: B-0 wt%, C-2 wt%, D-4 wt%, E-6 wt%, F-8 wt%, G-10 wt%.

property of composites begins to decline. This may be due to the enhanced amount of primary particles and the inhomogeneous dispersion of OMMT as increasing OMMT content, which leads to increased defects number. These make PLS nanocomposite cannot maintain its initial shape in the process of combustion and result in the decline of thermal resistance.

### 3.5. Mechanical properties

Flexural test was performed according to the GB/T1040—92 by WDS Electronic tensile testing machines, the loading rate was 2 mm/min. Compression test was performed according to the GB1041—79 by WDW-11 computer-controlled electronic universal testing machine, the loading rate was 5 mm/min. The results are showed in Table 1.

The tensile and compressive tests were carried out to examine the influence of the inclusion of organoclay on the mechanical properties of nanocomposites. Effects of organo-MMT content on the tensile strength and compressive strength of nanocomposites are described in Table 1. The presence of organoclay substantially increases the tensile strength and compressive strength in all composites relative to the pure silicone despite the small amounts of true clay existing in these systems. These enhancements are directly attributable to the reinforcement provided by the dispersed silicate nanolayers. The nanocomposite, containing 6 wt% OMMT, has the best mechanical performance with tensile strength of 6.264 MPa, which is five times more than that of pure silicone. When the nanocomposite contains 4–6 wt% OMMT, the maximal compressive strength is 11.503 MPa, which is about four times bigger than that of pure silicone. The mechanical properties stop increasing when OMMT content is over 6 wt% and then decline with increased OMMT content. In silicone matrix, the primary OMMT particles and the intercalated OMMT particles exist at the same time. The silicone chains which intercalated into OMMT layers are limited by the dipole interaction and space restriction of OMMT layers, which results in the enhancement of tensile and compressive strength and the decrease of elongation at break of composites. The sheet OMMT particles slip by external force along the force-oriented direction, which can play a similar role of plasticizer to increase mechanical properties of nanocomposites. Similar to the decline of temperature resistance, the decrease of mechanical properties may be also due to the enhanced amount of primary particles and the inhomogeneous dispersion of OMMT as increasing OMMT content, which leads to increased defects number. These defects are prone to resulting in stress concentration and leading to strength decreasing.

## 4. Conclusions

Organoclay was prepared by intercalating ammonium cations of CTAB through an ion exchange process. Phenylmethylsilicone/OMMT nanocomposites were prepared by in-situ intercalative polymerization. A morphological hierarchy was characterized by XRD, SEM and TEM spectra. Mechanical properties, high temperature resistance and barrier performance for water were also studied. The results show that silicone chains have inserted into the MMT layers, and the interlayer distance of MMT is expanded effectively after polymerization of phenylmethylsilicone prepolymer and methyl methacrylate, even forming exfoliated nanocomposites. OMMT content plays a great effect on the temperature resistance and mechanical properties of nanocomposites. The silicone/OMMT nanocomposite which containing 8 wt% OMMT has excellent temperature resistance with low thermal weight loss of 25% at 750 °C. The presence of organoclay substantially increases the tensile strength and compressive strength in all composites relative to the pure silicone. The temperature resistance, the barrier property for water and the mechanical properties of silicone/OMMT nanocomposite which prepared by in-situ intercalative polymerization are markedly improved.

**Table 1**
Mechanical properties of PLS nanocomposites with different OMMT content.

| OMMT content/wt% | 0 | 2 | 4 | 6 | 8 | 10 |
|---|---|---|---|---|---|---|
| Tensile strength/MPa | 1.247 | 1.846 | 5.446 | 6.264 | 3.751 | 3.171 |
| Elongation/% | 2.65 | 2.24 | 2.10 | 1.85 | 1.72 | 1.51 |
| Compressive strength/MPa | 2.834 | 3.786 | 11.503 | 10.767 | 9.362 | 5.652 |

## Acknowledgements

The work was supported by National Natural Science Foundation of China (20207003, 20704019), Major Program from the Science and Technology Council of Zhejiang Province and Jiangsu University Foundation for Excellent Young Teacher. The authors wish to express their appreciation to the Analytical Center at Jiangsu University for the analyses of SEM, XRD and TEM.

## References

Akat, H., Tasdelen, M. A., Prez, F. D., & Yagci, Y. (2008). Synthesis and characterization of polymer/clay nanocomposites by intercalated chain transfer agent. *European Polymer Journal, 44*, 1949–1954.

Chiu, F. C., Lai, S. M., Chen, Y. L., & Lee, T. H. (2005). Investigation on the polyamide6/organoclay nanocmposites with or without a maleated polyolefin elastomer as a tougher. *Polymer, 46*, 11600–11609.

Dasari, A., Yu, Z. Z., & Mai, Y. W. (2005). Effect of blending sequence on microstructure of ternary nanocomposites. *Polymer, 46*, 5986–5991.

Deshmane, C., Yuan, Q., & Misra, R. D. K. (2007). High strength–toughness combination of melt intercalated nanoclay-reinforced thermoplastic olefins. *Materials Science & Engineering, A: Structural Materials: Properties, Microstructure and Processing, 460–461*, 277–287.

Dong, W. F., Zhang, X. H., Liu, Y. Q., Gui, H., Wang, Q. G., Gao, J. M., et al. (2006). Effect of rubber on properties of nylon-6/unmodified clay/rubber nanocomposites. *European Polymer Journal, 42*, 2515–2522.

Fornnes, T. D., & Paul, D. R. (2003). Modeling properties of nylon 6/clay nanocomposites using composite theories. *Polymer, 44*, 4993–5013.

Gao, D. Y., Robert, B. H., Berthod, T., & Li, H. (2005). Studies on the structure of poly(acrylamide)/montmorillonite nanocomposite. *Polymeric Materials Science and Engineering, 21*, 201–205.

Homminga, D., Goderis, B., Dolbnya, I., & Groeninckx, G. (2006). Crystallization behavior of polymer/montmorillonite nanocomposites. Part II. Intercalated poly(ε-caprolactone)/montmorillonite nanocomposites. *Polymer, 47*, 1620–1629.

Huang, M. F., Yu, J. G., & Ma, X. F. (2006). High mechanical performance MMT-urea and formamide-plasticized thermoplastic cornstarch biodegradable nanocomposites. *Carbohydrate Polymers, 63*, 393–399.

Huskic, M., & Zigon, M. (2007). PMMA/MMT nanocomposites prepared by one-step in situ intercalative solution polymerization. *European Polymer Journal, 43*, 4891–4897.

Incarnato, L., Scarfato, P., Scatteia, L., & Acierno, D. (2004). Rheological behavior of new melt compounded copolyamide nanocomposites. *Polymer, 45*, 3487–3496.

Kaneko, M. L. Q. A., & Yoshida, I. V. P. (2008). Effect of natural and organically modified montmorillonite clays on the properties of polydimethylsiloxane rubber. *Journal of Applied Polymer Science, 108*, 2587–2596.

Kim, E. S., Kim, E. J., Shim, J. H., & Yoon, J. S. (2008). Thermal stability and ablation properties of silicone rubber composites. *Journal of Applied Polymer Science, 110*, 1263–1270.

Kojima, Y., Usuki, A., Kawasumi, M., Okada, A., Fukushima, Y., Karauchi, T., et al. (1993). Mechanical properties of nylon 6-clay hybrid. *Journal of Materials Research, 8*, 1185–1189.

Luo, J. J., & Daniel, I. M. (2003). Characterization and modeling of mechanical behavior of polymer/clay nancomposites. *Composites Science and Technology, 63*, 1607–1616.

Morgana, A. B., & Harrisb, J. D. (2004). Exfoliated polystyrener clay nanocomposites synthesized by solvent blending with sonication. *Polymer, 45*, 8695–8703.

Qi, Z. N., & Shang, W. Y. (2002). *Polymer/layered silicate nanocomposites theory and practice*. Beijing: Chemical Industry Press.

Salahuddin, N. A. (2004). Layered silicate/epoxy nanocomposites: Synthesis, characterization and properties. *Polymers for Advanced Technologies, 15*, 251–259.

Usuki, A., Kojima, Y., Kawasumi, M., Okada, A., Fukushima, Y., Kurauchi, T., et al. (1993). Synthesis of nylon 6-clay hybrid. *Journal of Materials Research, 8*, 1179–1184.

Wagener, R., & Reisinger, T. J. G. (2003). A rheological method to compare the degree of exfoliation of nanocomposites. *Polymer, 44*, 7513–7518.

Yang, I. K., & Hu, C. C. (2006). Preparation and rheological characterization of poly(*n*-butyl methacrylate)/montmorillonite composites. *European Polymer Journal, 42*, 402–409.

Yuan, Q., & Misra, R. D. K. (2006). Impact fracture behavior of clay-reinforced polypropylene nanocomposites. *Polymer, 47*, 4421–4433.

Zanetti, M., Lomakin, S., & Camino, G. (2000). Polymer layered silicate nanocomposites. *Macromolecular Materials and Engineering, 279*, 1–9.